New Journal and we have not received input yet 24 (2021) 100956

Contents lists available at ScienceDirect

Thermal Science and Engineering Progress

journal homepage: www.sciencedirect.com/journal/thermal-science-and-engineering-progress

# Electropolymerised molecularly imprinted polymers for the heat-transfer based detection of microorganisms: A proof-of-concept study using yeast

O. Jamieson [a], K. Betlem [b], N. Mansouri [b], R.D. Crapnell [b], F.S. Vieira [c], A. Hudson [a], C.E. Banks [b], C.M. Liauw [d], J. Gruber [e], M. Zubko [b], K.A. Whitehead [d], M. Peeters [a,*]

[a] Newcastle University, School of Engineering, Merz Court, Claremont Road, NE1 7RU Newcastle Upon Tyne, United Kingdom
[b] Manchester Metropolitan University, Faculty of Science and Engineering, John Dalton Building, Chester Street, M1 5GD Manchester, United Kingdom
[c] Departamento de Engenharia Química, Escola Politécnica, Universidade de São Paulo, Av. Prof. Luciano Gualberto, trav. 3, 380, CEP 05508-900 São Paulo, SP, Brazil
[d] Microbiology at Interfaces, Manchester Metropolitan University, John Dalton Building, Chester Street, M15GD Manchester, United Kingdom
[e] Departamento de Química Fundamental, Instituto de Química, Universidade de São Paulo, Av. Prof. Lineu Prestes, 748, CEP 05508-000 São Paulo, SP, Brazil

ARTICLE INFO

*Keywords:*
Heat-transfer
Electropolymerisation
Yeast
*Saccharomyces cerevisiae*
Microorganisms
Biomimetic sensors
Molecularly Imprinted Polymers (MIPs)
Heat-transfer method (HTM)

ABSTRACT

In this contribution, molecularly imprinted polymers (MIPs) were electropolymerised onto screen-printed carbon electrodes (SPCEs) to develop specific sensors for thermal detection of yeast. A laboratory yeast strain free of interferents was used to optimise the polymerisation procedure, whereas yeast in a complex mixture (yeast for baking) was employed to produce the final sensors and demonstrate proof-of-application. Two different electropolymerisation methods were employed, cyclic voltammetry and chronoamperometry respectively; the electrochemical methodology allows for controlled deposition and the ability to tailor the polymer surface to the required application. Infrared spectroscopy and scanning electron microscopy confirmed that the methods led to different structures; with cyclic voltammetry a high surface area was achieved, whereas for chronoamperometry a dense film was formed. Subsequently, these functionalised electrodes were inserted into a home-made thermal device that can measure the selective binding of yeast cells to the MIP layer *via* monitoring the thermal resistance ($R_{th}$) at the solid–liquid interface.

The results of the measurements showed that MIP-functionalised electrodes produced, according to both methods, a significant response in thermal signal for the MIP-functionalised electrode, which was not the case for the reference Non-Imprinted Polymer (NIP)-functionalised electrode. This demonstrated that thermal analysis can be employed for the detection of yeast, even in a complex sample such as food. To our knowledge, this is the first report of MIPs electropolymerised onto screen-printed electrodes for the thermal detection of fungi.

The proposed approach enables the fast production of low-cost electrodes using a simple manufacturing procedure compatible with a portable device, implying high commercial potential. In the future, this could be adapted to a broad range of microorganisms including bacteria.

## 1. Introduction

Microbiological contamination presents huge concerns in a wide variety of sectors throughout the world, such as in food and drink [1,2], sports [3], medicine [4] and even the construction industry [5]. Contamination of food and drink products specifically presents huge concerns for both health and economic reasons [6]. Even in developed economies foodborne illness is commonplace, with an estimated one third of populations suffering from a type of foodborne illness annually [7]. The quality and safety of food is best preserved by delaying the growth of specific bacteria or by reducing contamination by bacterial pathogens; therefore rapid detection and removal of infected foodstuff is vital [8]. The majority of current detection methods for microorganisms are based on microbiological techniques, analytical antibody assays and nucleic acid-based assays, such as the polymerase chain reaction (PCR) tests [9]. All these methodologies require time-consuming preparation, procedures and/or measurement protocols, thus, development of a fast, reliable, on-site sensor platform for the recognition of microorganisms is of high interest to the analytical community. Commonly, antibodies are used as a recognition element in sensor development due to the specific

* Corresponding author.
*E-mail address:* marloes.peeters@ncl.ac.uk (M. Peeters).

https://doi.org/10.1016/j.tsep.2021.100956
Received 14 January 2021; Received in revised form 20 April 2021; Accepted 29 April 2021
Available online 3 May 2021

recognition between the antibody and the target antigen, which can be released by, (*e.g.* virulence factors) or is present on the surface of the microorganism [10,11]. However, problems with antibody-based sensors include high cost, high batch-to-batch variation, limited stability, and the fact that some antibodies still require animals for production [12–14].

As such, for use in a portable sensor, molecularly imprinted polymers (MIPs) have gained significant interest as biomimetic recognition elements capable of replacing antibodies due to their high affinity, low production cost and superior chemical and thermal stability [15–17]. They can be produced using a wide range of monomers and synthetic methodologies, leading to a vast array of sensitive and selective recognition elements [18,19]. They have been shown to produce highly specific sensing platforms in conjunction with optical [20], electrochemical [21] and thermal [22] detection methodologies. MIPs epitomise versatility in respect to target sensing. With optimisation, they can be utilised for the detection of a significant breadth of targets, ranging from small molecules to proteins and cells [23].Whilst the present study demonstrates detection of yeast, there is promise to extrapolate the protocol to other targets, potentially even antimicrobial resistant (AMR) bacteria, in a bid to fight the critical issues posed by AMR. Thermal detection strategies have been relatively unexplored; when simply measuring the temperature such as with thermistors, it is difficult to require the level of specificity required for biomarker sensing. However, there has been promise in using the Heat-Transfer Method (HTM) which detection principle is based on measuring changes in heat transfer at the solid–liquid interface due to its low-cost, fast analysis, and ability to measure different markers by changing the functionalised interface. MIPs can be combined with the HTM as a read-out technique and have been shown to produce sensor platforms suitable for the detection of small molecules [24] and proteins [25,26], as well as for the monitoring of the growth of microorganisms such as yeast and *Staphylococcus aureus* in nutrient rich media [27,28]. Quantitative detection of microorganisms based on analysis of heat-transfer at the solid-interface provides significant challenges due to the inherent differences in size and shape of the microorganisms within a population. The selective detection of the presence of yeast cells has been reported previously using surface imprinted polymers (SIPs) combined with HTM [29,30]. One significant drawback of using these SIPs is the production time, which can take as long as 18 h. In this manuscript, we explore the use of electropolymerisation which significantly reduces the manufacturing process of the biosensor to minutes, in addition to forming the MIP layer directly onto the surface of the transducer [31]. There have been multiple reports on conductive and non-conducive polymer MIPs for various transducers including glassy carbon electrodes (GCE) [32–34], gold [35–37] and screen-printed carbon electrodes (SPCE) [38–40]. The latter are attractive options due to the ability to mass produce such sensors, in addition to their reliability, flexibility and low-cost [41,42]. Previously, we have shown that SPCEs can be used as substrates for the deposition of MIP particles for the detection of antibiotics [43] or have the MIP microparticles directly incorporated into the screen-printing ink [44]. Polypyrrole (PPy) is a commonplace monomer when considering the application of MIP synthesis in respect to electrochemical means due to its conductivity. Ramanavicius *et. al* [45] displayed the use of PPy for a detection sensor for bisphenol S through the use of functionalised glass. The produced polymers displayed sensitivity as low as 0.7–12.5 μm and displayed promising selectivity trends when compared to related compounds such as bisphenol C. The use of electrochemical polymerisation over oxidation polymerisation is favoured due to ease and speed of the synthesis process in addition to facilitating direct deposition onto conductive surfaces [46]. The imprinting of larger biomacromolecules, including proteins and microorganisms, can be complicated since these contain a myriad of potential binding sites. Hence, it is often required to use combination of monomers to achieve selective binding, which can be a time-consuming process without the use of computational modelling tools. Different strategies to develop MIPs for electrochemical sensing of biomarkers and larger macromolecules are discussed in Ref. [47].

In this manuscript we present a proof-of-concept that MIPs can be generated directly onto SPCE substrates using electropolymerisation for the detection of microorganisms, in this case yeast, using the HTM. Due to the low-cost and reproducible nature of the SPCEs, there is scope to use them as disposable sensors in the future for screening of contaminants in the food and water industry.

## 2. Experimental

### 2.1. Reagents

To optimise the synthesis procedure, we worked with *Saccharomyces cerevisiae* laboratory strain DLY640 originating from the Rothstein lab [48,49] which has the advantages of not containing interferents such as sorbitan monostereate and ascorbic acid in commercial baker's yeast. These compounds significantly interfere with analysis and mask the yeast and/or polymer signal and therefore a "pure" laboratory strain was used to optimise the synthesis procedure and enabling analysis with infrared (IR) spectroscopy and scanning electron microscopy (SEM). For each experiment, a fresh yeast colony was grown from a yeast extract peptone dextrose (YEPD) agar plate in 250 mL of YEPD broth until an optical density (OD) of at least 1.4 at 660 nm was reached. The optical density for cell concentration was determined by UV–vis analysis which was carried out on a Jenway 7205 UV–visible 72 Series Diode Array Scanning Spectrophotometer (UK). Allinson's Easy Bake Yeast (UK), containing *Saccharomyces cerevisiae* (7 g per sachet), sorbitan monostearate as emulsifier, and ascorbic acid as flour treatment agent, was used for all thermal analysis experiments to evaluate yeast detection in a complex sample such as food. Suspensions of yeast were prepared in sterile deionised water solutions, where the concentration was estimated using the optical density at 660 nm [50].

An optimal profilometer (Omniscan, UK) which uses a MicroXAM (phase shift) surface mapping microscope with an ADE phase shift (XYZ 4400 mL system) and an AD phase shift controller (Omniscan, UK) was used to determine layer thickness. This system was coupled to image analysis software Mapview AE (Omniscan, UK).

SPCEs were produced according to a well-known procedure described in [41]. Carbon-graphite ink formulation (Product Code: C2000802P2; Gwent Electronic Materials Ltd, UK) was printed onto a standard polyester substrate and cured at 60 °C for 30 min, followed by a dielectric layer (Product Code: D2070423D5; Gwent Electronic Materials Ltd., Pontypool, United Kingdom) to cover the connections, which was also cured at 60 °C for 30 min. The pyrrole was sourced from Acros Organics (Loughborough, UK), the yeast extract, peptone bacteriological agar bacteriological (AgarNO.1), D (+)-glucose and glycerol were all obtained from Fisher Scientific (Basingstoke, UK), while the adenine sulfate was purchased from Alfa Aesar (Heysham, United Kingdom). All other chemicals mentioned were acquired from Sigma Aldrich (Gillingham, UK). All experiments were carried out at 21 ± 1 °C (ambient temperature) unless noted differently. For polymerisation, a modified PBS solution (pH = 2) was used to ensure a constant iconic strength was maintained for all experiments. All other experiments were carried out in deionised water.

### 2.2. MIP and NIP syntheses

MIPs and NIPs were produced by electrodeposition. A solution of pyrrole (1 mM) in a phosphate buffered saline solution at pH = 2 was prepared as follows: 4 g of NaCl, 0.1225 g of KCl, 0.72 g of $Na_2HPO_4$ and 0.12 g of $KH_2PO_4$ were dissolved in 25 mL of deionised water (resistivity 18.2 MΩ cm). The solution was then acidified to pH 2 via the addition of dilute HCl.

Yeast cells were re-suspended in 2 mL of this solution to the density of approximately $5.0 \times 10^6$ colony forming units (CFU)/mL [28]. For the

"real" yeast sample, powder from Allinson's Easy Bake Yeast was suspended into deionised water solutions and the suspension density was determined spectrophotometrically as described in item 2.1. As the yeast was specialised for use in the culinary sector, it had other additives to enhance its performance. The addition of these additives complicates determination of the yeast cell concentration. Prior to using the *Saccharomyces cerevisiae* laboratory strain DLY640 it was recovered from cryo-storage on a YEPD plate. Then a single colony was re-suspended in 250 mL of YEPD broth and grown at, 23.00 ± 0.05 °C (for approx. 48 h) to an optical density of at least 1.4 at 660 nm. After growth, the yeast cells were washed 3 times with fresh YEPD, aliquoted into 2 mL samples containing 20% of glycerol which serves as a cryo-protector and stored at −80 °C.

All electrochemical experiments were performed using a three-electrode set up controlled by a PalmSens4 Potentiostat (the Netherlands), where the working electrode was an SPCE (diameter = 3.1 mm), counter electrode was a nickel wire and the reference was an external Ag|AgCl reference electrode. The procedures were all performed at 21 ± 1 °C in solutions made with deionised water (resistivity no less than 18 MΩ cm). The SPCE was placed in the acidified pyrrole PBS solution and polymerised according to two electrochemical methods. The first method was cyclic voltammetry, where the electrodes were placed in solution and cycled from – 0.2 V to + 1.2 V at 0.1 V $s^{-1}$ for 10 scans. The second method was chronoamperometry, where the potential was set to + 0.98 V and maintained for 100 s for polymerisation.

The polymerised SPCEs were placed under running hot water to remove yeast cells from the polymer complex, SEM analysis was carried out to confirm this method of extraction was sufficient (see Supporting Information S-1). SEM measurements were recorded on a Supra 40VP Field Emission from Carl Zeiss Ltd. (Cambridge, UK) with an average vacuum chamber of $1.3 \times 10^{-5}$ mbar and average gun vacuum of $1 \times 10^{-9}$ mbar. To enhance the contrast of these images, a thin layer of Au/Pd (8 V, 30 s) was sputtered onto the electrodes with a SCP7640 from Polaron (Hertfordshire, UK). Furthermore, references (Non-Imprinted Polymers) were prepared in a similar manner except there was no addition of yeast to the pyrrole solution in PBS. Diffuse reflectance Fourier transform infrared spectroscopy (DRIFTS) was conducted to monitor polymerisation over time; the high roughness and dark colour of the electrode surfaces made them suitable for DRIFTS. A Thermo-Nicolet Nexus FTIR, (DTGS detector), fitted with a Spectra-Tech DRIFTS cell (equivalent to the current Thermo-Fisher Scientific Collector™ II Diffuse Reflectance Accessory) was used for this analysis. Spectra were made up of 164 scans with resolution set to 4 $cm^{-1}$. The thickness of the polymerised film (a measure of the extent of pyrrole polymerisation) on the electrode was proportional to the absorbance of the N–H stretching band at 1600 $cm^{-1}$.

### 2.3. HTM measurements of yeast with MIP-modified SPEs

The Molecularly Imprinted Polymers polymerised SPEs (MIP-modified SPEs) were cut into squares (1 × 1 $cm^2$) around the working electrode. These were pressed onto a copper block and mounted into a 3D printed flow cell with an inner volume of 110 μL that was designed in house, where a glass slide of the same size was used to create a seal. This cell was sealed off with an O-ring and connected to the HTM set up that is described by van Grinsven *et al.* [51]. The copper block, which serves as a heat sink, is actively steered with a Proportional-Integral-Derivative (PID) controller. PID parameters can significantly affect the response recorded and therefore were kept at constant, optimised values of P = 1, I = 14, D = 0.3 [26].

The thermal resistance ($R_{th}$ – Eq. (1)) at the solid–liquid interface was calculated by subtracting the controlled input temperature of the copper block ($T_1$) from the temperature of the solution $T_2$, measured at 1.7 mm above the electrode surface, divided by the power (P) given to the heat source to maintain the required experimental temperature. The temperature in the liquid ($T_2$) was measured every second with a type K thermocouple at 1.7 mm above the chip surface.

$$R_{th} = \frac{T_1 - T_2}{P} \quad (1)$$

**Equation (1)-** Description of how to calculate the thermal resistance

Previous research has shown that changes at the solid–liquid interface result in a change in $R_{th}$. In the case of MIPs, the "pore blocking model" [52] demonstrates how binding of the target to the cavities in the polymer leads to an increase in $R_{th}$. All experiments were conducted at 37 ± 0.02 °C, except for one experiment carried out at 50.00 ± 0.02 °C to determine if higher temperatures increase binding to the surface (Supporting Information S-2). However, no significant change in the measured $R_{th}$ was found which could be due to disintegration of the yeast at elevated temperatures [28].

The MIP-modified SPE were stabilised in PBS for at least 45 min after which a second injection of PBS was performed to establish a stable baseline. Subsequently, at 30 min intervals, suspensions of increasing yeast concentrations ($1.0 \times 10^2$, $1.0 \times 10^3$, $1.0 \times 10^4$, $1.0 \times 10^5$, $1.0 \times 10^6$ and $1.0 \times 10^7$ CFU/mL) in deionised water were added into the flow cell with an automated NE500 programmable syringe pump (Prosense, Oosterhout, the Netherlands). The solutions were injected at intervals of 30 min, with an injection volume of 3 mL being injected with a flow rate of 1.975 mm/min. The thermal resistance was monitored over time and determined at each concentration. This was used to construct dose–response curves, where the limit of detection was calculated using the three-sigma method in the linear range of the sensor. To establish the specificity of the sensor platform, identical measurements were performed with a NIP-modified SPE.

## 3. Results

### 3.1. IR and SEM analyses to determine surface structure of MIP-modified SPEs

Firstly, the formation and deposition of PPy on the surface of the electrode material was investigated. The substrate of choice for the final sensor platform was a SPCE; however, this substrate is notoriously difficult to analyse due to its large, rough surface area and high absorbance. Therefore, to analyse the initial deposition technique, it was first performed using a gold substrate. PPy layers were formed on this substrate using chronoamperometry for different periods of time (0, 30, 60 and 120 s) to monitor the growth of the polymer layer. This was achieved by placing the electrode in the solution specified above and held at + 0.98 V *vs.* Ag|AgCl for the specified amount of time. The FTIR spectra for the different polymerisation times is presented in Fig. 1 A, where the increase in the peak at 1600 $cm^{-1}$, corresponding to N–H stretching, confirms an increase in the amount of PPy on the surface of the electrode. The IR absorption bands of the electrode composition (e.g. the ester carbonyl stretch of the binder at ca. 1730 $cm^{-1}$) are unaffected by the PPy [53]. As expected, the longer the system was subjected to the potential, the thicker the layer of PPy formed on the surface as seen by the increase in absorbance of the peak.

To obtain an estimate for the thickness of the layer of PPy, an Au electrode was coated with PPy and placed under a White Light Profilometer (Fig. 1B). While the binding kinetics for Au electrodes and SPCEs are different, this provided an indication of the layer thickness which is needed to bind the microbial cells but not too high so it hampers mass diffusion.

As seen in Fig. 1 B, the layer was non-uniform, manifesting a rough texture and an estimated thickness between 1.5 and 3 μm. It is reasonable to assume that the thickness of the layer deposited on an SPE would be thinner than this due to the slower electrode kinetics [54]. Yeast cells typically range from 5 to 10 μm in size [55], therefore a slightly longer deposition time of 100 s was chosen for sensing experiments. This would allow for the formation of cavities roughly 50% of the size of the yeast

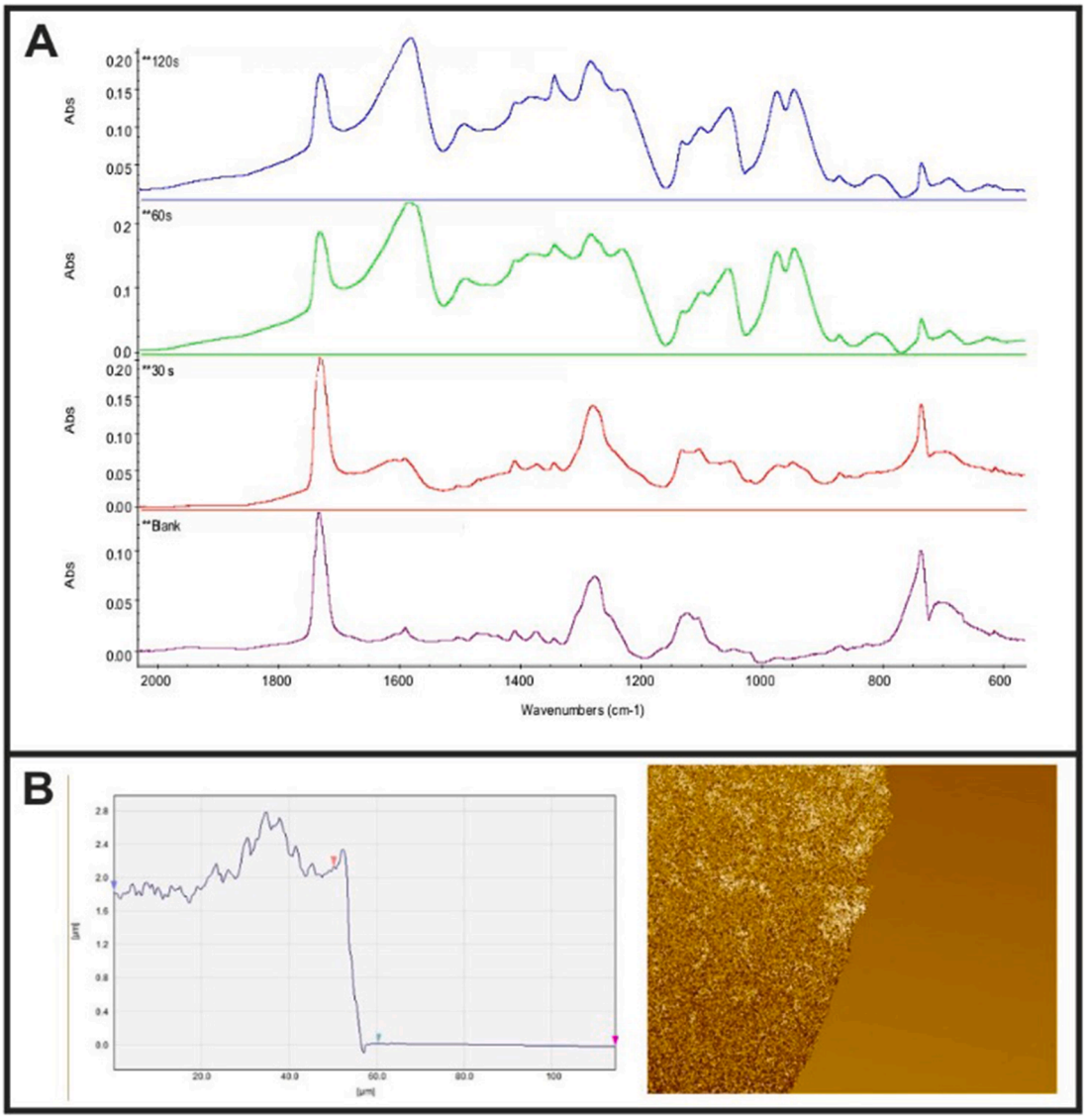


**Fig. 1.** A) FTIR result showing the generation of PPy on the surface of the electrode. B) White light profilometry of the PPy layer generated on the surface of the electrode.

cells, suggesting that they would not be fully covered by polymer. It was important to keep the polymer layer as thin as possible, whilst still offering binding sites for yeast that were deep enough for the yeast to bind to through both size, shape and functionality. Therefore, both cyclic voltammetric and chronoamperometric deposition methodologies were performed and compared, Fig. 2.

As can be seen in Fig. 2, there were significant differences observed in the polymeric coverage when using cyclic voltammetry (CV) and chronoamperometry (CA). When using CV, Fig. 2A, the formation of PPy on the surface begins following the oxidation of the pyrrole monomer on the first scan. The formation of PPy can be tracked by following the decrease in the current on the oxidation scan due to the polymerisation of monomeric pyrrole into polypyrrole. This was confirmed *via* SEM, Fig. 2B, where patches of polymer can be seen although there is not a uniform coverage across the SPE surface. In comparison, when using CA, Fig. 2C, a greater coverage of polymer was observed on the surface, Fig. 2D. This was expected as while CA is run, polymer was continuously formed since it is at the oxidation potential; however, when CV was used the polymer was only formed when the potential was raised above the required oxidation potential of the monomer [56]. Both of these polymer systems were then used for the detection of yeast cells. This preparation method, whilst presently being used for thermal detection, could be suitable for electrochemical detection such as electrochemical impedance spectroscopy or differential pulse voltammetry. However, it has to be noted that thick layers are needed for microorganism detection which can hamper electrochemical detection and thermal analysis we can make use of the full surface, including the non-conductive binder, which is expected to enhance the signal response.

### 3.2. *Thermal resistance measurements for yeast using MIP-modified SPCEs*

HTM allows for the monitoring of changes occurring at the solid–liquid interface through the change in measured thermal resistance. As such, PPy formed *via* both CV and CA imprinted with yeast cells was electrochemically deposited on the surface of SPCEs as described above; after which, the yeast cells were removed leaving specific associated cavities. SPCEs were chosen as the substrate for these sensing experiments as they offer ease of preparation for the MIPs due to the inclusion of counter and reference electrode in addition to a significant reduction in cost compared to other commonly used electrodes such as gold and glassy carbon. The functionalised SPCEs were then inserted into the flow

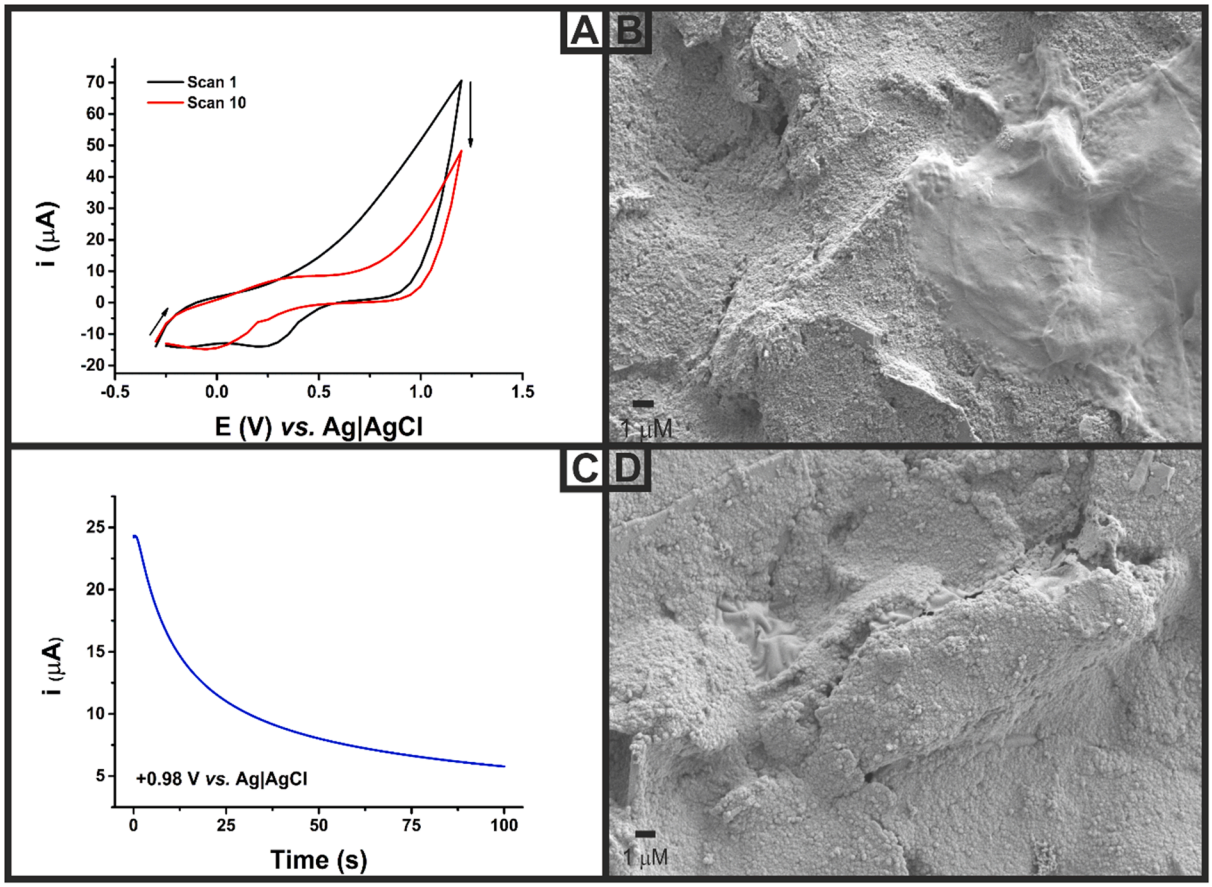


**Fig. 2.** A) Cyclic voltammograms for the formation of PPy on the surface of the SPCE performed at 100 mV $s^{-1}$. B) SEM image for the formation of PPy patches on the surface of the SPCE using cyclic voltammetry. C) Chronoamperommogram for the formation of a PPy layer on the surface of an SPCE at + 0.98 V *vs* Ag|AgCl for 100 s. D) SEM image for the formation of a PPy layer on the surface of an SPCE using chronoamperometry.

cell presented in Fig. 3 A and sealed with a rubber O-ring and copper block. The copper block temperature was set to 37 ± 0.02 °C, in line with previous studies on proteins and real-time monitoring of organisms [26,27]. To demonstrate proof-of-concept, a MIP-modified electrode produced with *Saccharomyces cerevisiae* laboratory strain DLY640 was measured (Supporting Information S-3). The electrode was stabilised in a buffered solution after which a suspension of *Saccharomyces cerevisiae* in PBS (1.0x$10^7$ CFU/mL) was added. A sharp increase in the thermal resistance was observed, which is due to binding of the yeast cells on the surface. Washing with the buffered solution did not change the signal, indicating that the yeast cells were firmly bound into cavities.

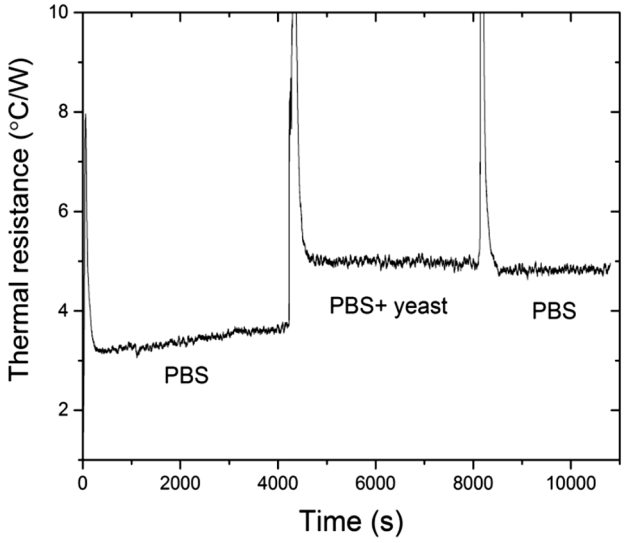


**Fig. 3.** A MIP-modified electrode (prepared with laboratory strain of yeast) was mounted into the HTM set up and stabilised in a standard PBS solution (pH = 7.4). While there is some minor drift in the signal, addition of a suspension of yeast (1.0 × 107 CFU/mL) in PBS led to a significant increase in the thermal resistance due to binding of yeast in the activities on the surface. This provided proof-of-concept and in following experiments, yeast from a complex mixture was considered.

Subsequently, we moved towards the yeast in a complex sample to further evaluate the specificity of the sensor platform. Initially, comparisons in the sensing proficiency for both the CV and CA MIPs were explored. An initial test was carried out to draft any initial insight to the function of the detection system. Fig. 3 displays a simplistic sample run of a single injection of complex yeast solution (followed by a PBS washing injection). A significant increase in thermal resistance gave a indiczation that the yeast adhered to the polymer and thus provided the first demonstration of the systems abilities.

The same procedure was used for both systems. The MIP SPE is mounted onto an O ring which upon the flow chamber, a copper block acting as the heat sink is placed on top and screwed in to consolidate the seal on the flow chamber. A blank solution of deionised water was injected to fill the flow cell, and the system allowed to reach a stable temperature for 45 min. The baseline $R_{th}$ value was calculated from the average of the final 600 data points (10 min) prior to the injection of the first concentration of yeast cells. Following this 3 mL of the lowest concentration of yeast cells ($10^2$ CFU/mL) was injected into the flow cell, indicated by the sharp vertical line in the raw data plots in Fig. 4.

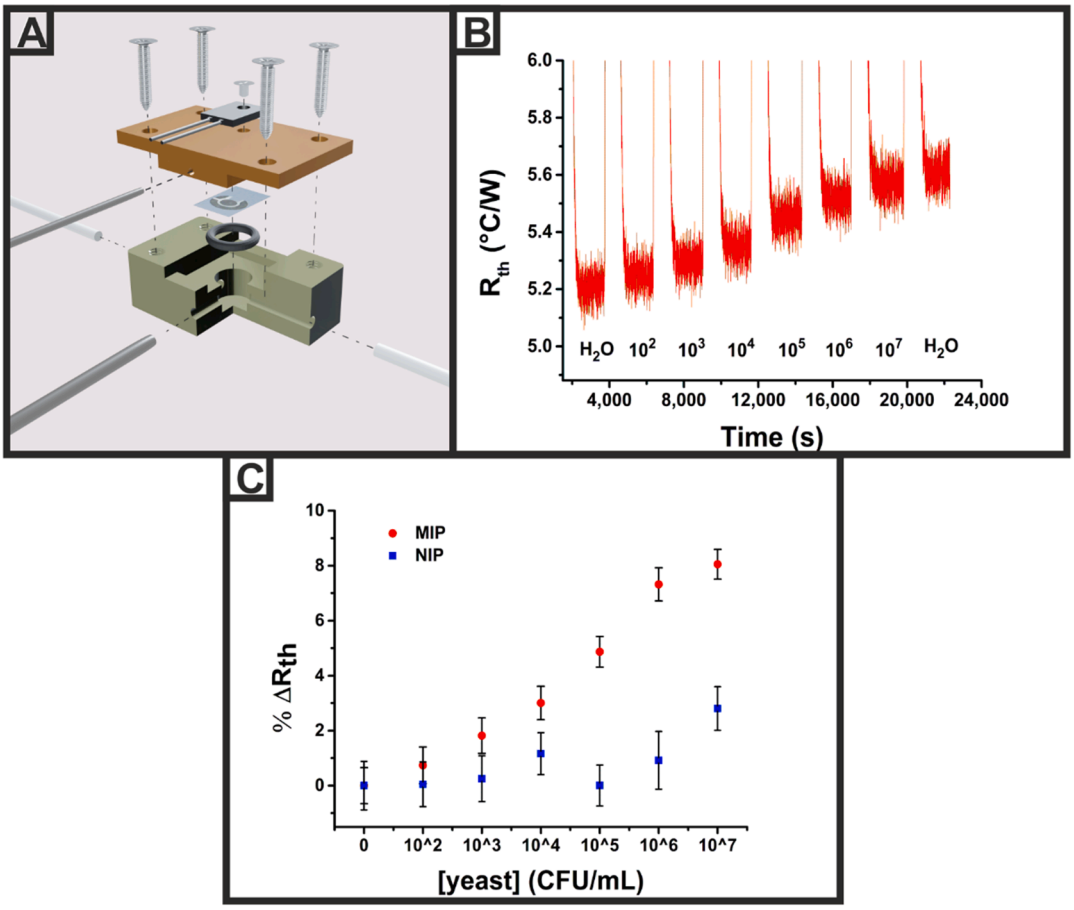


**Fig. 4.** A) Schematic diagram of the flow cell used throughout the thermal measurements in this work, comprising of a single thermocouple inserted into a main chamber with a flow inlet and outlet. B) HTM raw data plot of the measured $R_{th}$ *versus* the time for sequential additions of yeast cells ($10^2$-$10^7$ CFU/mL) to a MIP-coated SPCE produced using CV. C) Plot of the change in measured $R_{th}$ against the concentration of added yeast cells to a HTM set-up with both a MIP and NIP coated SPE.

This sharp increase in the $R_{th}$ was due to the injection of room temperature liquid (~20 °C) into the system at 37 °C. After the injection was completed, the $R_{th}$ was left to stabilise for 30 min before the next injection of analyte, thus facilitating calculation of the $R_{th}$ from the last 600 data points of each stabilisation period.

For the CV based MIP the baseline stabilised at a value of calculated to be 5.20 ± 0.03 °C/W. After the addition of yeast cells ($1\,0^2$) CFU/mL the measured $R_{th}$ increased to 5.24 ± 0.03 °C/W. It continued to rise after further additions of yeast cells in higher concentrations, which was attributed to the binding of yeast cells to the MIP layer on the SPE surface, making transfer of heat across the interface polymer/solution more difficult. For the final addition of yeast to the system, $R_{th}$ reached 5.61 ± 0.03 °C/W which represents an overall increase of 8 ± 1% in the $R_{th}$. Then, the system was injected with a blank solution of DI water and no significant increase in the measured $R_{th}$ (5.62 ± 0.03 °C/W). This indicated that the change in the $R_{th}$ was due to the presence of yeast cells binding to the MIP layer on the SPE and that washing with water did not cause a significant amount of yeast cells to be removed. An image obtained with the white light profilometer is shown in Supporting Information S-4, demonstrating the presence of yeast on the surface after HTM measurements with a MIP-modified electrode.

In contrast to this, the NIP-modified electrode showed little changes in the measured $R_{th}$ for any injection of yeast into the flow cell, Fig. 3C, up to $10^6$ CFU/mL. This indicated that the binding of yeast cells to the electrode surface was specific for the MIP platform and did not rely on non-specific adsorption to the surface of the polymer.

In comparison to the CV prepared platform, when CA was used the baseline stabilised at a value of 6.49 ± 0.03 °C/W, which was a higher value than that seen for CV based MIPs. This was expected due to the thicker, more uniform coverage of polymer across the SPCE surface increasing the resistance to heat-transfer across the system. For the MIP, there was an increase in the $R_{th}$ for every addition of increased concentration of yeast until the final addition of $10^7$ CFU/mL where the $R_{th}$ stabilised at a value of 6.87 ± 0.04 °C/W. In the case of the NIP, there was an initial rise in the measured $R_{th}$; however, this then reduced back to the baseline level.

Further indication of yeast binding can be gained from Fig. 5, an image captured from a white light profilometer clearly shows yeast cells upon the surface of the MIP. This image being capture after the final injection of PBS shows that the yeast cells are not merely settled upon the surface but bonded to it.Fig. 6.

Both the CV and CA production methods produced a system capable of detecting the presence of yeast in the system when the MIP was present and showed minimal or no response when the NIP was present. The CV produced system exhibited a higher specificity between MIP and NIP, where the limit of detection was determined at the three-sigma method. For the system with CV, a limit of detection was determined of 10^ 1.25 ± 0.09 CFU/mL, whereas this compared to a limit of detection of 10^ 1.12 ± 0.07 CFU/mL for CA, which are well below the concentrations found in the brewing process of ~ 10^4–10^6 CFU/mL [57]. The data in Fig. 4B confirm that at low concentrations the response is similar whereas the polymers produced using CV have higher response at higher concentration, suggesting a higher binding capacity. This could be due to higher surface area of the electrodes produced in this

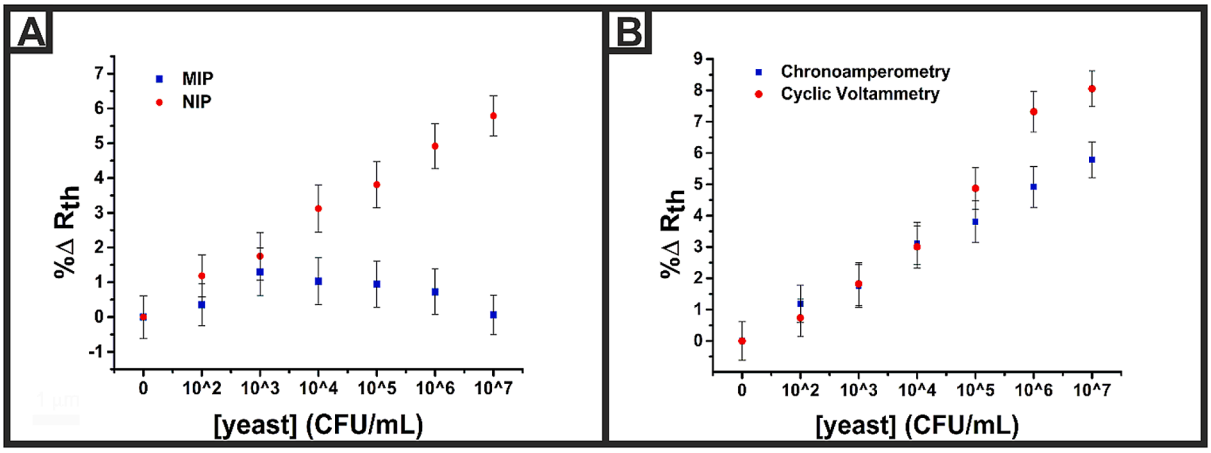


**Fig. 5.** A) Plot of the percentage change in the measured $R_{th}$ against the concentration of added yeast cells to a HTM set-up with both a MIP and NIP coated SPCE using chronoamperometry. B) Plot comparing the percentage change in $R_{th}$ for the MIP platforms produced by chronoamperometry and cyclic voltammetry. Error bars relate to the standard deviation of the experiment.

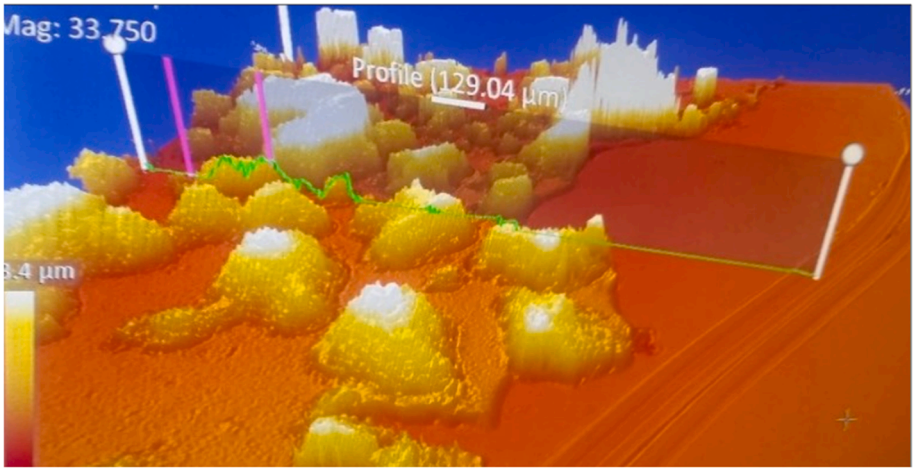


**Fig. 6.** Measurements with the white light profilometer of a MIP-modified electrode after HTM measurements confirmed the presence of yeast on the surface.

manner, although for detection of macromolecules it would normally be preferred to have a dense layer covering the surface to minimise non-specific binding by similar microorganisms or interferents from the matrix structure. Issues associated with MIP synthesis for larger biomolecules has been widely reported on. Whether it is the challenges faced by protein imprinting due to their poor structural resilience and restricted synthetic routes [47] or the obstacles of cell (e.g. yeast) imprinting such as the complexity and fragility of cells, coupled with their fluidity [58]. This study joins the founding insight into the future ease of application of MIPs to templates of a significantly larger size and more complex physical state. In the future, more work on understanding the surface structure of electropolymerised MIPs is needed to understand how it impacts on the specificity and selectivity of binding of macromolecules.

## 4. Conclusions

MIPs and reference NIPs for the detection of yeast were deposited onto SPCEs using cyclic voltammetry and chronoamperometry. To optimise the synthesis procedure, MIPs were prepared using at *Saccharomyces cerevisiae* laboratory strain DLY640 which is free from interferents, allowing to study the layer thickness and surface structure by using IR and SEM analysis. It was shown that with cyclic voltammetry a "patch-type" structure was formed, with polymer mainly forming around the ridges of the SPCEs. In contrast, if CA was used, a thick homogeneous coating was formed with an estimated layer thickness of several microns, which is sufficient to incorporate the yeast cells. SPCEs coated with both methods were mounted into our home-made thermal device, where the response of the thermal signal was used to monitor binding of yeast from a commercial baker's yeast sample (Allinson's Easy Bake) to demonstrate proof-of-concept. A significant response in the thermal resistance was observed from the MIP, contrary to reference NIP electrodes, demonstrating the change in signal was due to binding of yeast in the imprinted cavities. Electrodeposition of MIPs onto the SPCEs led to sensors with similar levels of detection attained,; however, the polymers produced using CA had a higher binding capacity. These levels of detection are within the relevant range in the brewing industry, suitable for in-situ monitoring in fermenters, or to determine the yeast presence in food samples [59]. This preparation method could be suitable for electrochemical detection such as EIS (along with pore blocking theory) or using DPV. The change in electrochemical impedance or reduction in obtained signal using other methods will be highly dependant on many factors not only layer thickness (electrolyte, deposition method, electrode, adhesion all play roles). This means the thermal detection method Is more flexible and requires less optimisation. Could just mention that a comparison could be interesting for future work. The advantage of the method proposed in this project is that it is fast, low-cost, and portable, providing it with high commercial

potential, and demonstrating that analysis of heat-transfer analysis can play a vital role in the biosensor community. Due to the versatility of the molecular imprinting technology, in the future this can be expanded to other relevant objects such as macromolecules, bacteria and eukaryotic cells which will open many other applications beyond the food industry.

## Declaration of Competing Interest

The authors declare that they have no known competing financial interests or personal relationships that could have appeared to influence the work reported in this paper.

## Acknowledgements

We would like to acknowledge the EPSRC (EP/R029296/1) for salary of Dr Hudson and Dr Foster for production of the SPEs. JG thanks Conselho Nacional de Desenvolvimento Científico e Tecnológico (CNPq) (Proc. n° 424027/2018-6 and 307501/2019-1) for financial support.

## Appendix A. Supplementary data

Supplementary data to this article can be found online at https://doi.org/10.1016/j.tsep.2021.100956.

## References

[1] S. Pedley, G. Howard, The public health implications of microbiological contamination of groundwater, Q. J. Eng. Geol. Hydrogeol. 30 (2) (1997) 179–188.
[2] Y. Wadamori, R. Gooneratne, M.A. Hussain, Outbreaks and factors influencing microbiological contamination of fresh produce, J. Sci. Food Agric. 97 (5) (2017) 1396–1403.
[3] C. Dacarro, A. Picco, P. Grisoli, M. Rodolfi, Determination of aerial microbiological contamination in scholastic sports environments, J. Appl. Microbiol. 95 (5) (2003) 904–912.
[4] L. Kallings, O. Ringertz, L. Silverstolpe, Microbiological contamination of medical preparations, Acta Pharmaceutica Suecica 3 (3) (1966) 219.
[5] N.S. Geweely, Evaluation of ozone for preventing fungal influenced corrosion of reinforced concrete bridges over the River Nile, Egypt, Biodegradation 22 (2) (2011) 243–252.
[6] S. Magnússon, H. Gunnlaugsdóttir, H. van Loveren, F. Holm, N. Kalogeras, O. Leino, J. Luteijn, G. Odekerken, M. Pohjola, M. Tijhuis, State of the art in benefit–risk analysis: food microbiology, Food Chem. Toxicol. 50 (1) (2012) 33–39.
[7] S. Akhtar, M.R. Sarker, A. Hossain, Microbiological food safety: a dilemma of developing societies, Crit. Rev. Microbiol. 40 (4) (2014) 348–359.
[8] J. Gruber, H.M. Nascimento, E.Y. Yamauchi, R.W. Li, C.H. Esteves, G.P. Rehder, C. C. Gaylarde, M.A. Shirakawa, A conductive polymer based electronic nose for early detection of Penicillium digitatum in post-harvest oranges, Mater. Sci. Eng., C 33 (5) (2013) 2766–2769.
[9] P.D. Skottrup, M. Nicolaisen, A.F. Justesen, Towards on-site pathogen detection using antibody-based sensors, Biosens. Bioelectron. 24 (3) (2008) 339–348.
[10] F.S. Felix, L. Angnes, Electrochemical immunosensors–a powerful tool for analytical applications, Biosens. Bioelectron. 102 (2018) 470–478.
[11] O.A. Sadik, J.M. Van Emon, Applications of electrochemical immunosensors to environmental monitoring, Biosens. Bioelectron. 11 (8) (1996) i–x.
[12] S. Banta, K. Dooley, O. Shur, Replacing antibodies: engineering new binding proteins, Annu. Rev. Biomed. Eng. 15 (2013) 93–113.
[13] A.C. Gray, A.R. Bradbury, A. Knappik, A. Plückthun, C.A. Borrebaeck, S. Dübel, Animal-derived-antibody generation faces strict reform in accordance with European Union policy on animal use, Nat. Methods 17 (8) (2020) 755–756.
[14] J. Wackerlig, P.A. Lieberzeit, Molecularly imprinted polymer nanoparticles in chemical sensing–synthesis, characterisation and application, Sens. Actuators, B 207 (2015) 144–157.
[15] M. Jia, Z. Zhang, J. Li, X. Ma, L. Chen, X. Yang, Molecular imprinting technology for microorganism analysis, TrAC, Trends Anal. Chem. 106 (2018) 190–201.
[16] J.W. Lowdon, H. Diliën, P. Singla, M. Peeters, T.J. Cleij, B. van Grinsven, K. Eersels, MIPs for commercial application in low-cost sensors and assays–an overview of the current Status Quo, Sens. Actuators B: Chem. (2020) 128973.
[17] K. Haupt, K. Mosbach, Molecularly imprinted polymers and their use in biomimetic sensors, Chem. Rev. 100 (7) (2000) 2495–2504.
[18] J.J. BelBruno, Molecularly imprinted polymers, Chem. Rev. 119 (1) (2018) 94–119.
[19] B. Sellergren, A.J. Hall, Molecularly imprinted polymers, Supramolecular chemistry: from molecules to nanomaterials, (2012).
[20] A. Rico-Yuste, S. Carrasco, Molecularly imprinted polymer-based hybrid materials for the development of optical sensors, Polymers 11 (7) (2019) 1173.
[21] R. Gui, H. Jin, H. Guo, Z. Wang, Recent advances and future prospects in molecularly imprinted polymers-based electrochemical biosensors, Biosens. Bioelectron. 100 (2018) 56–70.
[22] H. Diliën, M. Peeters, J. Royakkers, J. Harings, P. Cornelis, P. Wagner, E. Steen Redeker, C.E. Banks, K. Eersels, B. van Grinsven, Label-free detection of small organic molecules by molecularly imprinted polymer functionalized thermocouples: toward in vivo applications, ACS Sens. 2 (4) (2017) 583–589.
[23] S. Ansari, Combination of molecularly imprinted polymers and carbon nanomaterials as a versatile biosensing tool in sample analysis: recent applications and challenges, TrAC, Trends Anal. Chem. 93 (2017) 134–151.
[24] K. Betlem, I. Mahmood, R. Seixas, I. Sadiki, R. Raimbault, C. Foster, R. Crapnell, S. Tedesco, C. Banks, J. Gruber, Evaluating the temperature dependence of heat-transfer based detection: a case study with caffeine and Molecularly Imprinted Polymers as synthetic receptors, Chem. Eng. J. 359 (2019) 505–517.
[25] F. Canfarotta, J. Czulak, K. Betlem, A. Sachdeva, K. Eersels, B. Van Grinsven, T. Cleij, M. Peeters, A novel thermal detection method based on molecularly imprinted nanoparticles as recognition elements, Nanoscale 10 (4) (2018) 2081–2089.
[26] R.D. Crapnell, F. Canfarotta, J. Czulak, R. Johnson, K. Betlem, F. Mecozzi, M. P. Down, K. Eersels, B. van Grinsven, T.J. Cleij, Thermal detection of cardiac biomarkers heart-fatty acid binding protein and ST2 using a molecularly imprinted nanoparticle-based multiplex sensor platform, ACS Sens. 4 (10) (2019) 2838–2845.
[27] K. Betlem, A. Kaur, A.D. Hudson, R.D. Crapnell, G. Hurst, P. Singla, M. Zubko, S. Tedesco, C.E. Banks, K. Whitehead, Heat-transfer method: a thermal analysis technique for the real-time monitoring of Staphylococcus aureus growth in buffered solutions and digestate samples, ACS Appl. Bio Mater. 2 (9) (2019) 3790–3798.
[28] K. Betlem, S. Hoksbergen, N. Mansouri, M. Down, P. Losada-Pérez, K. Eersels, B. Van Grinsven, T.J. Cleij, P. Kelly, D. Sawtell, Real-time analysis of microbial growth by means of the Heat-Transfer Method (HTM) using Saccharomyces cerevisiae as model organism, Phys. Med. 6 (2018) 1–8.
[29] D. Yongabi, M. Khorshid, P. Losada-Pérez, K. Eersels, O. Deschaume, J. D'Haen, C. Bartic, J. Hooyberghs, R. Thoelen, M. Wübbenhorst, Cell detection by surface imprinted polymers SIPs: a study to unravel the recognition mechanisms, Sens. Actuators, B 255 (2018) 907–917.
[30] O. Hayden, F.L. Dickert, Selective microorganism detection with cell surface imprinted polymers, Adv. Mater. 13 (19) (2001) 1480–1483.
[31] R.D. Crapnell A. Hudson C.W. Foster K. Eersels B.v. Grinsven, T.J. Cleij, C.E. Banks, M. Peeters, Recent advances in electrosynthesized molecularly imprinted polymer sensing platforms for bioanalyte detection Sensors 19(5) (2019) 1204.
[32] V.K. Gupta, M.L. Yola, N. Özaltın, N. Atar, Z. Üstündağ, L. Uzun, Molecular imprinted polypyrrole modified glassy carbon electrode for the determination of tobramycin, Electrochim. Acta 112 (2013) 37–43.
[33] E. Mathieu-Scheers, S. Bouden, C. Grillot, J. Nicolle, F. Warmont, V. Bertagna, B. Cagnon, C. Vautrin-Ul, Trace anthracene electrochemical detection based on electropolymerized-molecularly imprinted polypyrrole modified glassy carbon electrode, J. Electroanal. Chem. 848 (2019), 113253.
[34] Y. Wu, P. Deng, Y. Tian, Z. Ding, G. Li, J. Liu, Z. Zuberi, Q. He, Rapid recognition and determination of tryptophan by carbon nanotubes and molecularly imprinted polymer-modified glassy carbon electrode, Bioelectrochemistry 131 (2020), 107393.
[35] L. Li, L. Yang, Z. Xing, X. Lu, X. Kan, Surface molecularly imprinted polymers-based electrochemical sensor for bovine hemoglobin recognition, Analyst 138 (22) (2013) 6962–6968.
[36] S. Menon, S. Jesny, K.G. Kumar, A voltammetric sensor for acetaminophen based on electropolymerized-molecularly imprinted poly (o-aminophenol) modified gold electrode, Talanta 179 (2018) 668–675.
[37] T. Wang, C. Shannon, Electrochemical sensors based on molecularly imprinted polymers grafted onto gold electrodes using click chemistry, Anal. Chim. Acta 708 (1–2) (2011) 37–43.
[38] R.A. Couto, S.S. Costa, B. Mounssef Jr, J.G. Pacheco, E. Fernandes, F. Carvalho, C. M. Rodrigues, C. Delerue-Matos, A.A. Braga, L.M. Goncalves, Electrochemical sensing of ecstasy with electropolymerized molecularly imprinted poly (o-phenylenediamine) polymer on the surface of disposable screen-printed carbon electrodes, Sens. Actuators, B 290 (2019) 378–386.
[39] V.M. Ekomo, C. Branger, R. Bikanga, A.-M. Florea, G. Istamboulie, C. Calas-Blanchard, T. Noguer, A. Sarbu, H. Brisset, Detection of Bisphenol A in aqueous medium by screen printed carbon electrodes incorporating electrochemical molecularly imprinted polymers, Biosens. Bioelectron. 112 (2018) 156–161.
[40] H. Zhang, G. Liu, C. Chai, A novel amperometric sensor based on screen-printed electrode modified with multi-walled carbon nanotubes and molecularly imprinted membrane for rapid determination of ractopamine in pig urine, Sens. Actuators, B 168 (2012) 103–110.
[41] C.W. Foster, J.P. Metters, D.K. Kampouris, C.E. Banks, Ultraflexible screen-printed graphitic electroanalytical sensing platforms, Electroanalysis 26 (2) (2014) 262–274.
[42] R.O. Kadara, N. Jenkinson, C.E. Banks, Characterization and fabrication of disposable screen printed microelectrodes, Electrochem. Commun. 11 (7) (2009) 1377–1380.
[43] O. Jamieson, T.C. Soares, B.A.d. Faria, A. Hudson, F. Mecozzi, S.J. Rowley-Neale, C.E. Banks, J. Gruber, K. Novakovic, M. Peeters, Screen printed electrode based detection systems for the antibiotic amoxicillin in aqueous samples utilising molecularly imprinted polymers as synthetic receptors, Chemosensors 8 (1) (2020) 5.
[44] S. Casadio, J. Lowdon, K. Betlem, J. Ueta, C.W. Foster, T. Cleij, B. van Grinsven, O. Sutcliffe, C.E. Banks, M. Peeters, Development of a novel flexible polymer-based biosensor platform for the thermal detection of noradrenaline in aqueous solutions, Chem. Eng. J. 315 (2017) 459–468.

[45] R. Viter, K. Kunene, P. Genys, D. Jevdokimovs, D. Erts, A. Sutka, K. Bisetty, A. Viksna, A. Ramanaviciene, A. Ramanavicius, Photoelectrochemical bisphenol S sensor based on ZnO-nanoroads modified by molecularly imprinted polypyrrole, Macromol. Chem. Phys. 221 (2) (2020) 1900232.
[46] S. Ramanavicius, A. Ramanavicius, Conducting polymers in the design of biosensors and biofuel cells, Polymers 13 (1) (2021) 49.
[47] R.D. Crapnell, N.C. Dempsey-Hibbert, M. Peeters, A. Tridente, C.E. Banks, Molecularly imprinted polymer based electrochemical biosensors: Overcoming the challenges of detecting vital biomarkers and speeding up diagnosis, Talanta Open (2020), 100018.
[48] J.S. Wood, L.H. Hartwell, A dependent pathway of gene functions leading to chromosome segregation in Saccharomyces cerevisiae, J. Cell Biol. 94 (3) (1982) 718–726.
[49] L. Maringele, D. Lydall, EXO1-dependent single-stranded DNA at telomeres activates subsets of DNA damage and spindle checkpoint pathways in budding yeast yku70Δ mutants, Genes Dev. 16 (15) (2002) 1919–1933.
[50] D. Burke, D. Dawson, T. Stearns, Methods in Yeast Genetics: A Cold Spring Harbor Laboratory Course Manual, 2000 Edition, Cold Spring Harbor Laboratory Press. [Google Scholar], Plainview, NY, 2000.
[51] B. Van Grinsven, N. Vanden Bon, H. Strauven, L. Grieten, M. Murib, K.L. Jiménez Monroy, S.D. Janssens, K. Haenen, M.J. Schöning, V. Vermeeren, Heat-transfer resistance at solid–liquid interfaces: a tool for the detection of single-nucleotide polymorphisms in DNA, ACS Nano 6 (3) (2012) 2712–2721.
[52] M. Peeters, P. Csipai, B. Geerets, A. Weustenraed, B. Van Grinsven, R. Thoelen, J. Gruber, W. De Ceuninck, T. Cleij, F. Troost, Heat-transfer-based detection of L-nicotine, histamine, and serotonin using molecularly imprinted polymers as biomimetic receptors, Anal. Bioanal. Chem. 405 (20) (2013) 6453–6460.
[53] A. Yussuf, M. Al-Saleh, S. Al-Enezi, G. Abraham, Synthesis and characterization of conductive polypyrrole: the influence of the oxidants and monomer on the electrical, thermal, and morphological properties, Int. J. Polymer Sci. (2018).
[54] E.P. Randviir, A cross examination of electron transfer rate constants for carbon screen-printed electrodes using Electrochemical Impedance Spectroscopy and cyclic voltammetry, Electrochim. Acta 286 (2018) 179–186.
[55] M. Zakhartsev, M. Reuss, Cell size and morphological properties of yeast Saccharomyces cerevisiae in relation to growth temperature, FEMS Yeast Res. 18 (6) (2018) foy052.
[56] P.K. Sharma, G. Gupta, V.V. Singh, B. Tripathi, P. Pandey, M. Boopathi, B. Singh, R. Vijayaraghavan, Synthesis and characterization of polypyrrole by cyclic voltammetry at different scan rate and its use in electrochemical reduction of the simulant of nerve agents, Synth. Met. 160 (23–24) (2010) 2631–2637.
[57] F.B. Piló, E.J. Carvajal-Barriga, M.C. Guamán-Burneo, P. Portero-Barahona, A.M. M. Dias, L.F.D.d. Freitas, F.d.C.O. Gomes, C.A. Rosa, Saccharomyces cerevisiae populations and other yeasts associated with indigenous beers (chicha) of Ecuador, Braz. J. Microbiol. 49 (4) (2018) 808–815.
[58] J. Pan, W. Chen, Y. Ma, G. Pan, Molecularly imprinted polymers as receptor mimics for selective cell recognition, Chem. Soc. Rev. 47 (15) (2018) 5574–5587.
[59] L.R. Beuchat, Media for detecting and enumerating yeasts and moulds, Int. J. Food Microbiol. 17 (2) (1992) 145–158.